

# Dynamic Elastic Behavior of $\alpha$ -Satellite DNA Domains Visualized In Situ in Living Human Cells

Richard D. Shelby,\* Klaus M. Hahn,<sup>‡</sup> and Kevin F. Sullivan\*

\*Department of Cell Biology and <sup>‡</sup>Division of Virology, Department of Neuropharmacology, The Scripps Research Institute, La Jolla, California 92037

**Abstract.** We have constructed a fluorescent  $\alpha$ -satellite DNA-binding protein to explore the motile and mechanical properties of human centromeres. A fusion protein consisting of human CENP-B coupled to the green fluorescent protein (GFP) of *A. victoria* specifically targets to centromeres when expressed in human cells. Morphometric analysis revealed that the  $\alpha$ -satellite DNA domain bound by CENPB-GFP becomes elongated in mitosis in a microtubule-dependent fashion. Time lapse confocal microscopy in live mitotic cells revealed apparent elastic deformations of the central domain of the centromere that occurred during

metaphase chromosome oscillations. These observations demonstrate that the interior region of the centromere behaves as an elastic element that could play a role in the mechanoregulatory mechanisms recently identified at centromeres. Fluorescent labeling of centromeres revealed that they disperse throughout the nucleus in a nearly isometric expansion during chromosome decondensation in telophase and early G1. During interphase, centromeres were primarily stationary, although motility of individual or small groups of centromeres was occasionally observed at very slow rates of 7–10  $\mu\text{m}/\text{h}$ .

**C**ENTROMERES are the specialized genomic loci, present once on each chromosome, that encode the segregation function of the genome in mitosis and meiosis (Clarke and Carbon, 1980; Pluta et al., 1995). They accomplish this by directing the assembly of a dynamic mechanochemical complex consisting of the kinetochores formed at the surface of each sister chromatid and the central pairing domain in the chromosome interior (Earnshaw and Rattner, 1989). The kinetochores are the primary site of interaction of spindle microtubules with the chromosomes and possess microtubule binding, assembly modulating, and microtubule-dependent motor protein activities (Mitchison and Kirschner, 1985; Hyman and Mitchison, 1990, 1991; Lombillo et al., 1995). The central pairing domain links the replicated centromere into a single mechanical unit and contains a protease-sensitive linkage that is specifically cleaved to initiate anaphase chromosome segregation (Holloway et al., 1993; Stratmann and Lehner, 1996). These functions are integrated with the chromosome axis through a specialized form of chromatin, which in animal cells comprises the extensive satellite heterochromatin domain, spanning 400–5,000 kb of contiguous DNA along the chromosome fiber (Willard, 1991; Tyler-Smith and Willard, 1993).

The bipolar attachment of chromosomes to microtubules in the mitotic spindle results in net poleward forces that create tension across the centromeres, borne across this specialized centromeric chromatin (Roos, 1973; Nicklas, 1988). Evidence that mechanical tension across centromeres can modulate functions of the spindle has mounted steadily in recent years. Using elegant needle micromanipulation techniques to direct mechanical forces on chromosomes, Nicklas and colleagues first showed that tension is required for stable microtubule attachment to kinetochores (Ault and Nicklas, 1989; Nicklas and Ward, 1994). A role for tension in regulating force production by kinetochores was proposed by Skibbens and Salmon (1993, 1995) and their colleagues based upon video-enhanced DIC microscopy of chromosomes in mitotic newt lung epithelial cells (Skibbens et al., 1993, 1995). Finally, a key mechanism of mitosis, the one that ensures that all the chromosomes are properly engaged on the spindle before anaphase, has recently been proposed to involve a novel mechanosensory activity of the centromere (McIntosh, 1991). The first direct evidence that animal cells delay anaphase until all chromosomes have achieved bipolar attachment was provided by Rieder and colleagues, who proposed that anaphase onset is regulated by a negative signal generated by unattached kinetochores (Rieder et al., 1994, 1995). This mechanism has been directly linked to chromosome tension through chromosome micromanipulation experiments in insect spermatocytes arrested in metaphase I by improper assembly of a sex trivalent (Li and Nicklas,

Please address all correspondence to K.F. Sullivan, Department of Cell Biology, The Scripps Research Institute, 10666 Torrey Pines Rd., La Jolla, CA 92037. Tel.: (619) 784-2350. Fax: (619) 784-2345. E-mail: ksullivan@scripps.edu

1995). Metaphase arrest was relieved by tugging on the monopolar oriented chromosome to simulate bipolar spindle attachment, revealing a mechanical link to the anaphase checkpoint.

Taken together, these results establish a model of the centromere as a molecular tensiometer that functions, quite literally, at the center of the mitotic mechanism to convert mechanical stress into biological signals. An important correlation between mechanical force and the chemistry of the centromere has been identified through analysis of a kinetochore-associated phosphoprotein(s) recognized by a monoclonal antibody, 3F3 (Cyert et al., 1988; Gorbsky and Ricketts, 1993). 3F3 antigen(s) become phosphorylated in prophase and is progressively dephosphorylated after chromosome attachment and movement to the metaphase plate (Gorbsky and Ricketts, 1993). By combining micromanipulation of insect spermatocyte chromosomes with 3F3 immunostaining, it has been shown that tension exerted on the chromosome leads to dephosphorylation of kinetochore proteins, providing a direct link between tension and kinetochore chemistry (Nicklas et al., 1995). These experiments provide a clue as to how the centromere might be able to signal tension, but do not show how tension is actually detected. One important hypothesis is that the centromere contains proteins whose conformations are directly affected by mechanical stress, leading to changes in enzymatic or binding activities (McIntosh, 1991; Skibbens et al., 1993; Nicklas et al., 1995). These molecular events, however, occur in the context of a huge macromolecular complex that, in higher cells, is dominated by the extensive satellite heterochromatin domain of the centromere that provides the physical linkage between sister kinetochores. Indeed, while the sequence of centromere satellite DNA is evolutionarily unconserved, a unique form of chromatin structure has been found at all centromeres examined to date (Bloom et al., 1984; Polizzi and Clarke, 1991; Tyler-Smith and Willard, 1993).

One function of centromeric chromatin may be to provide a reproducible mechanical environment for the tensiometric mechanism(s) at the centromere. In this work we have investigated the dynamic mechanical and motile behaviors of centromeric chromatin in living cells by labeling a defined DNA sequence compartment within human centromeres. A fusion between human CENP-B (Earnshaw et al., 1987), a centromeric satellite DNA-binding protein, and *A. victoria* green fluorescent protein (GFP) (Chalfie et al., 1994), is efficiently incorporated into HeLa centromeres, at a level estimated to correspond to 300–3,000 molecules. Using time-lapse confocal microscopy, we find that human  $\alpha$ -satellite chromatin behaves as an elastic material during mitosis, increasing twofold in width along the spindle axis from prophase to metaphase. In highly resolved specimens, we observe reversible extensions of 200–400 nm that occur between sister  $\alpha$ -satellite domains during metaphase chromosome oscillations. These morphological chromatin dynamics require the presence of microtubules and thus appear to report directly on the tense status of centromeres within the spindle. In addition centromere positions and motility can be monitored in telophase and interphase nuclei. After an apparent isometric expansion that occurs in telophase and early G<sub>1</sub>, cen-

tromeres are generally stationary within the nucleus. Occasionally, however, selective motility of one or a few centromeres at a time is observed during interphase. Generation of human chromosomes labeled at a single locus by incorporation of CENPB-GFP provides new avenues for investigation of genomic structure and dynamics in the context of living cells.

## Materials and Methods

### Cell Culture and Transfection

HeLa (ATCC CCL3) and U2OS (ATCC HTB96) cells were maintained in DMEM with 10% FCS (Gibco-BRL, Gaithersburg, MD) at 37°C in a 5% CO<sub>2</sub> atmosphere. Cells were plated on glass coverslips at a density of  $2\text{--}2.5 \times 10^4$  cells/cm<sup>2</sup> the night before transfection. Transfection was performed in serum free medium using Lipofectamine (Gibco-BRL) as previously described (Sullivan et al., 1994). Cells were visualized by fluorescence microscopy 18–72 h following application of DNA.

### DNA Constructs

Wild-type GFP. This construct was assembled from three DNA fragments. The vector backbone was a 3.5-kb *Apal* and *SacI* fragment prepared from plasmid pCDL-CAHA1, which contains an enhanced SV40 early promoter driving a copy of the human CENP-A gene. The *Apal* site at CENP-A codon 2 is in frame with an identical site at codon 2 of CENP-B, so this vector provides the 5' untranslated region and start codon of CENP-A. The CENP-B portion of the construct extended from codon 2 to codon 169, and was synthesized by PCR, with the addition of an *XbaI* restriction site at the 3' end of the fragment for fusion with GFP. The GFP cDNA, including a short polylinker preceding the initiation codon for GFP, was obtained as a 1-kb *XbaI-SacI* restriction fragment from a plasmid, pGEX-GFP, kindly provided by J. Harper. (The Scripps Research Institute, La Jolla, CA.) These three fragments were ligated together to form pCENPB-GFP and plasmids were recovered by transformation into *E. coli*. All sequences amplified by PCR were sequenced after cloning to verify sequence fidelity (Sequenase, USB, Cleveland, OH). The mutant CENP-B sequence, CENP-B  $\Delta 4\text{--}16$ , contained a deletion of codons 4–16, produced by oligonucleotide directed mutagenesis. It was transferred to pCENPB-GFP as an *Apal-XhoI* fragment, replacing the corresponding region of the wild-type DNA-binding domain.

A second construct was prepared using the mutant S65T form of GFP, kindly provided by Drs. R. Heim and R. Tsien (University of California, San Diego, CA.) In this case, CENP-B and GFP fragments were amplified by PCR, incorporating the in frame *XbaI* site for fusion of CENP-B to GFP and the products were cloned directly into the CMV promoter vector pCDNA-3 (Invitrogen, San Diego, CA). The resulting plasmid, pCB-G(S65T), was checked for fidelity by DNA sequence analysis.

### Fluorescence and Immunofluorescence Microscopy

Cells were fixed for microscopy in PBS containing 4% formaldehyde prepared freshly from paraformaldehyde, washed three times with PBS, and then mounted with an anti-quenching reagent (SlowFade, Molecular Probes, Eugene, OR). Alternatively, coverslips could be simply washed in PBS and mounted directly on slides for observation within 10–15 min. Immunofluorescence was performed as described previously (Sullivan et al., 1994), using antibodies against tubulin (DM1A, Sigma Immunochemicals, St. Louis, MO), CENP-B (mACA-1; Earnshaw et al., 1987), a human centromere autoantiserum (hACA-M; Sullivan et al., 1994), or polyclonal rabbit sera against lamin-A, a gift from Dr. Larry Gerace (The Scripps Research Institute, La Jolla, CA), or CENP-E, a gift from Dr. Don Cleveland (University of California, San Diego, CA). For *in vivo* observation, coverslips were mounted with DMEM in a Dvorak-Stotler chamber (Nicholson Precision Instruments, Gaithersburg, MD) and an air curtain incubator was used to maintain the microscope stage between 35°C–37°C.

Images were collected on an MRC-600 confocal microscope built on a Zeiss Axiovert 100 inverted microscope using a 63 $\times$  1.4 NA Zeiss Neo Fluor lens and 10% laser power for illumination (Bio Rad Labs, Hercules,

1. Abbreviation used in this paper: GFP, green fluorescent protein.

CA). Confocal microscopy allowed identification of individual centromeres within the densely packed clusters of centromeres at metaphase and anaphase, which was not possible by standard epifluorescence microscopy. Single images from fixed and live specimens were collected by averaging 5–15 scans at the normal scan rate of the microscope,  $\sim 1$  s/scan. Optical section series were collected in the same mode with a step size of 0.36 or 0.54  $\mu\text{m}$ /section; 5 scans were averaged from living specimens, resulting in a 5-s image collection time. For time lapse sequences, images were obtained by averaging 2–4 scans in the fast scan mode (ca. 0.6 s/scan), for a collection time of 1.2–2.4s per image. The time required to store a full frame image to disk was  $\sim 6.5$  s, allowing a maximal collection rate of 6–7 images per minute. Time lapse segments were collected from a single focal plane at maximal rates during mitotic observations and at 0.5–2 frames per minute for interphase. One limitation of this method is the motion of centromeres in live cells during image acquisition. This is negligible for fast time lapse segments where centromeres moving at a rate of 2  $\mu\text{m}/\text{min}$  will only move  $\sim 0.1$   $\mu\text{m}$  during image formation. Similarly, in optical section series motion during image formation would be  $< 0.2$   $\mu\text{m}$ . However, successive images along the  $z$ -axis are offset by up to 15 s (0.5  $\mu\text{m}$ ). A second limitation encountered in time lapse observations is that centromeres sometimes move out of the focal plane, restricting the number of centromeres available for analysis.

Wide field optical section microscopy was performed using an Applied Precision (Mercer Island, WA) microscope system built on an Olympus IX-70 using a 60 $\times$  water immersion lens. After deconvolution, a projection image was constructed from the entire section series.

### Image Processing and Analysis

For quantitative morphometry and motility analysis, images were imported into an image processing program (Image Pro Plus, Media Cybernetics, Bethesda, MD). Outlines of individual centromeres were established by a thresholding algorithm and their dimensions were determined as the axes of an ellipse encompassing each signal. Images of optical section series were inspected visually to identify the section containing the maximal cross section of each centromere and morphological data were collected from that section. Centromere dimensions in each population approximated a normal distribution. The significance of morphological differences was evaluated with Student's  $t$  test. For motility analysis, time lapse image sequences were viewed as movies using Bio Rad Confocal Assistant software to identify centromeres that could be tracked through the sequence. Image stacks were then imported into Image Pro Plus and the positions of each centromere were recorded. For the experiment shown in Fig. 7, fixed points on either side of the metaphase plate were chosen at approximately the apex of an equilateral triangle whose base was drawn through the center of the chromosome band at anaphase. These fixed points were used to approximate the positions of the spindle poles for calculation of centromere-to-pole distances shown in Fig. 7 *b*. Data were exported to a spreadsheet (Excel, Microsoft Corporation, Redmond, WA) for analysis.

## Results

### Fluorescent Labeling of Human Centromeric DNA Sequences In Vivo

To develop a probe for centromere dynamics, we fused the coding region for the DNA-binding domain of CENP-B, codons 1–167 (Sullivan and Glass, 1991; Pluta et al., 1992; Yoda et al., 1992), to the  $\text{NH}_2$  terminus of the *A. victoria* GFP cDNA (Prasher et al., 1992; Chalfie et al., 1994), using PCR to introduce compatible restriction sites. When introduced into HeLa cells the chimeric gene produced a fluorescent protein, CENPB-GFP, that accumulated in numerous foci within the nuclei of transfected cells, readily visible in fixed (Fig. 1 *A*) or living specimens (Fig. 1 *B*). The identity of these labeled foci as centromeres was confirmed in two ways. First, a control construct was expressed using a mutated form of CENP-B, containing a small deletion that destroys DNA-binding activity (Pluta

et al., 1992; Yoda et al., 1992). The resulting protein, CENPB- $\Delta$ 416-GFP, accumulated throughout the nucleus, with some concentration in nucleoli, but failed to adopt a centromere-like localization (Fig. 1 *C*). Secondly, transfected cells were examined by immunofluorescence using human anti-centromere antibodies (Fig. 1 *D*) or a monoclonal antibody against CENP-B, mACA-1 (Earnshaw et al., 1987), that recognizes the COOH terminus of endogenous HeLa CENP-B (Fig. 1 *E*). In each case, CENPB-GFP labeled foci corresponded precisely to centromeres as defined by immunostaining. Thus, binding of  $\alpha$ -satellite DNA sequences by CENP-B targets GFP to human centromeres, rendering these loci visible in situ by fluorescence microscopy in living cells.

To determine whether CENPB-GFP can be used as a probe for centromere dynamics in vivo, cells transfected with CENPB-GFP were mounted in a culture chamber for observation by fluorescence microscopy using cooled CCD imaging. Mitotic cells with labeled centromeres were observed undergoing apparently normal chromosome segregation (Fig. 2 *A*). CENPB-GFP labeled cells were able to complete mitosis with normal cytokinesis during fluorescence observation (Fig. 2 *B*). The rate of chromosome separation in this cell was  $\sim 1$ –2  $\mu\text{m}$  per minute (Fig. 2 *C*), consistent with normal rates of anaphase in HeLa cells. Observation of cells in late telophase or early G1, still connected by a cytoplasmic bridge, confirms that cells expressing CENPB-GFP are able to successfully complete mitosis (see below). We conclude that expression of CENPB-GFP at levels sufficient for in vivo observation does not disrupt mitosis.

### Morphological Dynamics of $\alpha$ -Satellite DNA Domains in the Cell Cycle

Classic immunofluorescence experiments using human centromere autoantibodies revealed that centromeres become duplicated during G2 and are visible as paired spots throughout mitosis until the onset of anaphase (Brenner et al., 1981). However, immunofluorescence and immunoelectron microscopy with CENP-B antibodies demonstrated that CENP-B is distributed more uniformly across the entire heterochromatic domain in human chromosomes, with paired centromeres often unresolved on isolated mitotic chromosomes (Earnshaw et al., 1987; Cooke et al., 1990; Compton et al., 1991). In interphase cells CENPB-GFP was observed as single, symmetric fluorescent foci with some clustering around nucleoli or heterochromatic domains (Fig. 3 *A*). About 60 discrete foci of varying fluorescence intensity could be resolved in interphase nuclei, indicating that at least half of the centromeres in these highly aneuploid HeLa cells ( $2n = \sim 80$ ) are resolved as individual spots. Cells in prometaphase (Fig. 3 *B*) show an elongation of some centromeres, but we do not detect paired spots of CENPB-GFP fluorescence in HeLa cells until metaphase, where CENPB-GFP fluorescence is sometimes resolved into distinct twin foci but often appears as single elongated structures oriented parallel to the spindle axis, perpendicular to the metaphase plate (Fig. 3 *C*). In anaphase, CENPB-GFP foci return to their symmetric morphology (Fig. 3 *D*). The  $\alpha$ -satellite domain of the centromere appears to become elongated at a rela-

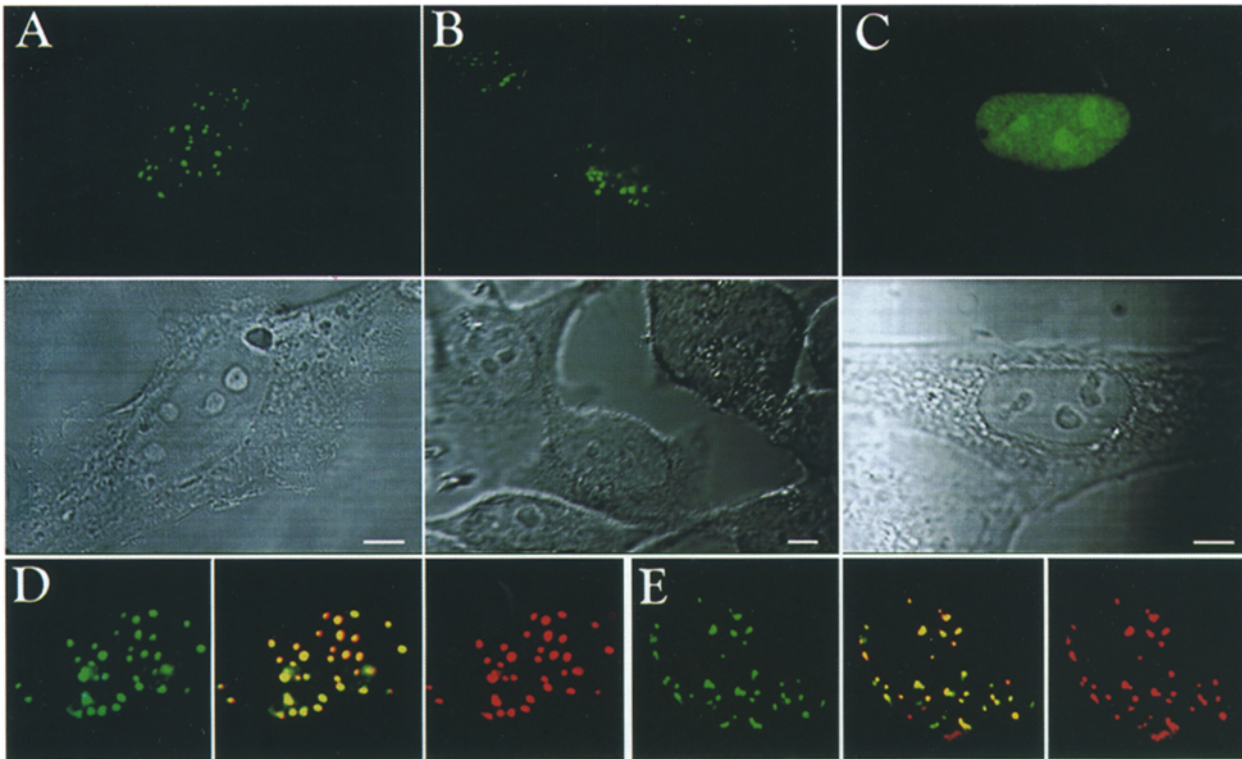


**Figure 1.** Targeting GFP to centromeric  $\alpha$ -satellite DNA. Cells were transfected with plasmid pCENPB-GFP and visualized 48 h later by confocal microscopy. (A) Fixed cell, 4% formaldehyde; (B) live cells; (C) GFP coupled to a mutant CENP-B DNA-binding domain that lacks DNA-binding activity failed to adopt a specific localization within the nucleus. Immunofluorescence confirms that the sites of CENPB-GFP localization correspond to centromeres. Transfected cells were fixed 48 h following transfection and subjected to immunofluorescence using (D) human anti-centromere antibodies or (E) monoclonal antibody mACA-1 against the COOH terminus of human CENP-B. In each panel the GFP signal is shown in green on the left while antibody signal detected with rhodamine is shown in red on the right. A merge of the two signals is shown in the center to evaluate codistribution, where yellow indicates signal overlap. Bars: (A–C) 5  $\mu$ m.

tively late stage during mitosis, temporally correlated with spindle attachment rather than centromere replication or chromosome condensation.

To examine the structural changes in  $\alpha$ -satellite domains during mitosis more accurately, we used dual-label immunofluorescence to simultaneously visualize centromeres and the nuclear lamina (Fig. 4, A–F). Immunofluorescence with mACA-1 allowed analysis of CENP-B in multiple cells without the complication of variable expression levels obtained using CENPB-GFP. It also allowed more consistent resolution of CENP-B domains into paired spots as compared with CENPB-GFP, which we believe is due to overexpression of CENPB-GFP, as discussed below. Visualization of lamin-A allowed us to accurately stage cells within mitosis. The largest cross section for each CENP-B signal within a cell was located in a complete optical section series and measured to determine centromere dimensions as the major and minor axes of an ellipse that contained the signal. The ratio of these axes,  $r_x$ , is a measure of the symmetry of the centromere profiles. A summary of these data are presented in Table I.

Cells in interphase had intact nuclear lamina with no detectable cytoplasmic lamin-A fluorescence and, as described above, CENP-B foci in these cells generally presented round, nearly symmetric profiles in optical sections (Fig. 4 A). Measurements from cells judged to be in G1 on

the basis of CENP-B signal intensity revealed a mean major axis length of 0.74  $\mu$ m (Table I). Cells in prophase had well defined nuclear lamina but also exhibited diffuse cytoplasmic and nucleoplasmic lamin-A fluorescence (Fig. 4 B). The mean major axis length of prophase  $\alpha$ -satellite domains, 0.85  $\mu$ m, was greater than interphase cells but they remain nearly symmetric single spots with an  $r_x$  of 1.4, the same as interphase cells. Only rarely (<10%) did prophase  $\alpha$ -satellite domains appear to resolve as a pair of spots in HeLa cells. Cells in prometaphase had bright cytoplasmic lamin-A staining and no, or almost no, remaining nuclear lamina and centromeres that had not yet congressed (Fig. 4 C). Prometaphase cells contained a mixture of symmetric and elongated  $\alpha$ -satellite domains, many of which could be resolved into closely apposed paired spots (arrows, Fig. 4 C), with a mean major axis length of 1.05  $\mu$ m. Metaphase was identified by virtue of a set of centromeres that had fully congressed to a metaphase plate (Fig. 4, D and E). In these cells, about half of the centromeres could be resolved with a classic paired dot morphology, possessing two separated sister CENP-B foci of equal intensity whose long axis was perpendicular to the metaphase plate. The mean major axis length of metaphase  $\alpha$ -satellite domains, corresponding to the width across the centromere, was 1.48  $\mu$ m. However, if only those centromeres that are actually resolved as pairs are considered, this mean length

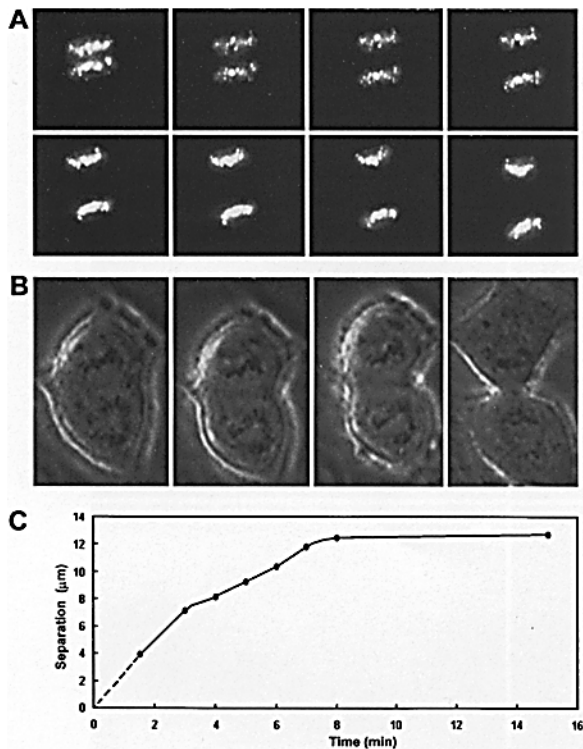


**Figure 2.** Mitosis is undisturbed in the presence of CENPB-GFP. HeLa cells were transfected with pCENPB-GFP and mounted in an incubation chamber  $\sim 48$  h later for live observation by fluorescence microscopy. A metaphase cell was identified and imaged using a cooled CCD camera at  $\sim 1$ -min intervals beginning just after anaphase onset. (A) Fluorescence images of GFP-labeled centromeres during anaphase, progressing from the upper left to lower right images. (B) Phase images taken during the latter half of the time course showing normal cytokinesis. (C) Centromere separation was determined as the distance between the centroids of each group of centromeres and is plotted as a function of time.

increased to  $1.60 \mu\text{m}$ . These differences in major axis length between successive mitotic stages are significant at a level of  $P < 0.001$  based on a Student's  $t$  test. After anaphase separation, centromeres returned to their compact, symmetric morphology with a mean major axis length of  $0.73 \mu\text{m}$ , identical to that measured in interphase cells.

These experiments demonstrate that inner domain of the centromere, defined by the CENP-B rich  $\alpha$ -satellite domains and the central pairing domain between them, undergoes an elongation beginning in prometaphase and reaching maximal extension at metaphase. We have also visualized this elongation by wide field optical section microscopy coupled with computational deconvolution (Hiraoka et al., 1990; Fig. 4, G–I). These images show a U2OS cell in metaphase, following transfection with CENPB-GFP (green) and immunofluorescence using an antibody to the kinetochore plate protein CENP-E (red). The extended nature of the  $\alpha$ -satellite domains is quite evident, as is the diminution of CENPB-GFP signal in the center of the centromere.

One possible explanation for these observations is that

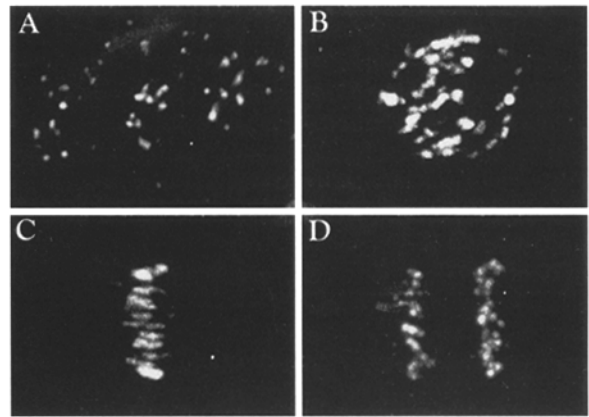


**Figure 3.** CENPB-GFP reveals morphological changes in  $\alpha$ -satellite domains during the cell cycle. HeLa cells expressing CENPB-GFP were fixed and analyzed by serial section confocal microscopy. A set of optical sections collected at  $0.36\text{-}\mu\text{m}$  intervals, spanning a total depth of  $2\text{--}5 \mu\text{m}$  through the optical axis was obtained from a group of representative cells in (A) interphase; (B) prometaphase; (C) metaphase; and (D) anaphase. Images are projections of three consecutive optical sections.

the centromeres do not elongate, but rather reorient at metaphase to become perpendicular to the optical axis, allowing maximal resolution in the image ( $x, y$ ) plane. Cells at other stages have centromeres that are, presumably, oriented randomly with respect to the optical ( $z$ ) axis. We have not made quantitative measurements along the  $z$  axis due to limitations in axial resolution inherent in fluorescence microscopy. However, we do not believe that differences in orientation significantly affect our findings, for two reasons. First, if prophase centromeres are extended along the  $z$  axis, we would expect that measurements made from projection images of multiple sections would be greater than single plane measurements, yet no differences were seen with  $1.4 \mu\text{m}$  projections. Second, if centromeres in prophase are morphologically equivalent to those in metaphase, many prophase centromeres should be oriented at an angle sufficient to see the paired dot morphology, which we did not observe. While reorientation of centromeres may contribute moderately to our results, there must be additional factors that lead to a physical increase in the distance across the centromere at metaphase.

#### **Disruption of Microtubules Inhibits Centromere Elongation**

Elongation of the  $\alpha$ -satellite domains could represent a late stage in the structural maturation of the centromeres or mitotic chromosomes, such as decatenation by topoisomerase II (Gimenez-Abian et al., 1995) or structural changes induced by assembly of other centromere proteins such as CENP-E or CENP-F (Yen et al., 1992; Liao et al., 1995). Alternatively, the elongated morphology of centromeres in metaphase could be a result of mitotic forces, reflecting the fact that chromosomes are under tension during most of mitosis (Nicklas, 1988). Since mitotic forces require microtubules, we sought to distinguish these two possibilities by examining  $\alpha$ -satellite morphology in cells arrested in mitosis with low concentrations of the microtu-

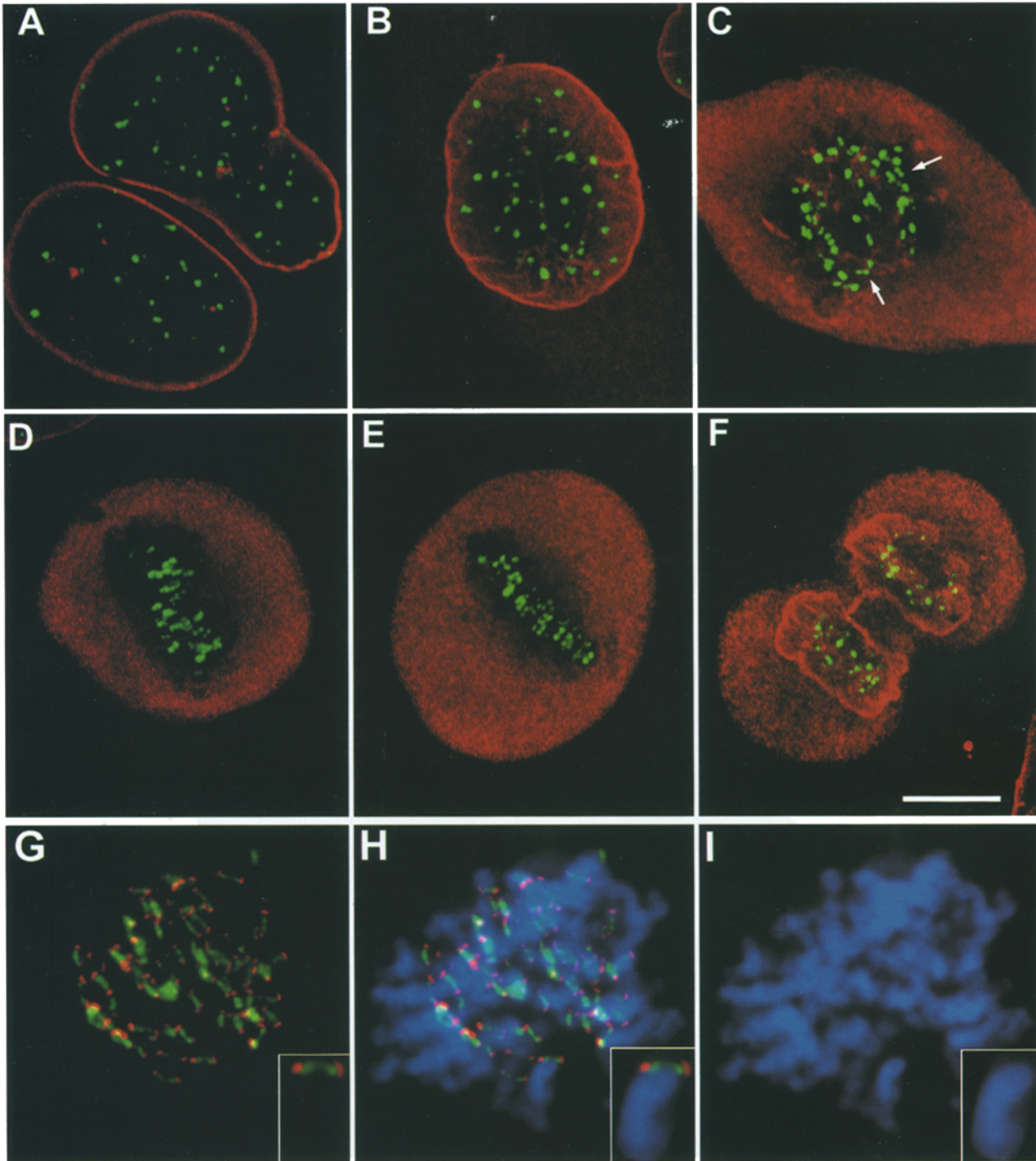


**Figure 4.** Morphology of CENP-B at different stages of mitosis. (A–F) HeLa cells were subject to immunofluorescence using anti-CENP-B monoclonal mACA-1 (green) and a rabbit antiserum against lamin-A (red). A complete optical section series was collected at 0.36- $\mu$ m intervals and used for the morphometric analysis summarized in Table I. Illustrated are cells in (A) interphase; (B) prophase; (C) prometaphase; (D and E) metaphase; and (F) telophase. Arrows in C indicate centromeres with paired dot morphology that first become visible during prometaphase. (G–I) U2OS cells were transfected with pCENPB-GFP (green) and then subjected to immunofluorescence with a rabbit antiserum against CENP-E (red). Chromosomes were counterstained with DAPI (blue). A cell in metaphase was imaged as an optical section series, subjected to deconvolution, and then a projection image of the complete cell was constructed. (G) Merge of CENPB-GFP and CENP-E highlights centromere structure; (H) three color images showing centromeres on the chromosomes; and (I) chromosomes alone. Bar, (F) 10  $\mu$ m.

Table 1.  $\alpha$ -Satellite Morphometry

	Interphase	Prophase	Prometaphase	Metaphase	Telophase
Major axis ( $\mu\text{m}$ )	$0.74 \pm 0.25$ (136)	$0.85 \pm 0.27$ (139)	$1.05 \pm 0.30$ (122)	$1.48 \pm 0.29$ (136)	$0.73 \pm 0.22$ (76)
Minor axis ( $\mu\text{m}$ )	$0.54 \pm 0.17$	$0.62 \pm 0.18$	$0.68 \pm 0.18$	$0.71 \pm 0.17$	$0.52 \pm 0.14$
Aspect ratio	$1.40 \pm 0.32$	$1.40 \pm 0.33$	$1.61 \pm 0.46$	$2.15 \pm 0.57$	$1.40 \pm 0.27$

Mean values  $\pm$  standard deviation for centromere dimensions and aspect ratio determined from cells, some of which are shown in Fig. 4. Numbers of individual centromeres in the analyzed populations are shown in parentheses.

bule disrupting agent vinblastine, to promote mitotic arrest without completely disrupting spindle structure (Wendell et al., 1993). At 10 nM vinblastine,  $\sim 40$ – $50\%$  of the cells were arrested in mitosis after 15 h as judged by chromosome condensation and a metaphase- or prometaphase-like distribution of centromeres. Numerous arrested cells, roughly half of the mitotic population, were observed with unelongated centromeres (Figs. 5, A, C, and F).

To ensure that the morphology observed in fixed specimens accurately reflects the *in vivo* distribution of CENPB-GFP, we used optical section confocal microscopy to analyze centromere morphology in live cells. Centromeres in a typical vinblastine-arrested metaphase cell were highly symmetric structures, loosely distributed around the central plane (Fig. 5 C). In contrast, centromeres in an untreated metaphase cell were distinctly elongated (Fig. 5 D). In this cell a pair of chromosomes that have either failed to congress or have separated early are located near the spindle poles, defining the axis of the mitotic spindle. Although this spindle is somewhat tilted, elongation of centromeres along the spindle axis is clear, particularly in individual cross sections. Measurement of eight centromeres in this cell that were distinctly resolved into paired dots resulted in a mean major axis length of  $1.67 \pm 0.15 \mu\text{m}$ . This was twice the length of the symmetric centromeres of the vinblastine arrested cell shown in Fig. 5 C, which had a mean major axis length of  $0.85 \pm 0.15 \mu\text{m}$ . A total of 72 centromeres were counted in this cell, representing  $\sim 90\%$  of the chromosome number of a HeLa cell, rendering unlikely the hypothesis that these cells with symmetric centromeres have simply undergone centromere splitting without segregation. Resolution of centromeres in live metaphase cells is potentially complicated by the motility of centromeres, which show characteristic poleward and antipoleward oscillations during metaphase, at rates of  $\sim 2 \mu\text{m}/\text{min}$  (Skibbens et al., 1993; and see below). However, individual images were collected within 5 s, during which time a maximum of only  $0.2 \mu\text{m}$  of motion may have occurred, insufficient to yield the observed difference in dimensions following treatment with vinblastine. Vinblastine is therefore a potent inhibitor of centromere elongation.

Despite the high proportion of vinblastine arrested cells that exhibited symmetric centromeres, a significant fraction, roughly half, display the elongated centromere morphology typical of normal metaphase cells. At very low levels ( $\sim 2 \text{ nM}$ ) of vinblastine, spindle organization in HeLa cells remains largely intact (Jordan et al., 1992; Wendell et al., 1993). In our experiments, approximately half of the cells retain vestiges of mitotic spindle organization as assayed by tubulin immunofluorescence. While the quality of immunofluorescence in cells transiently trans-

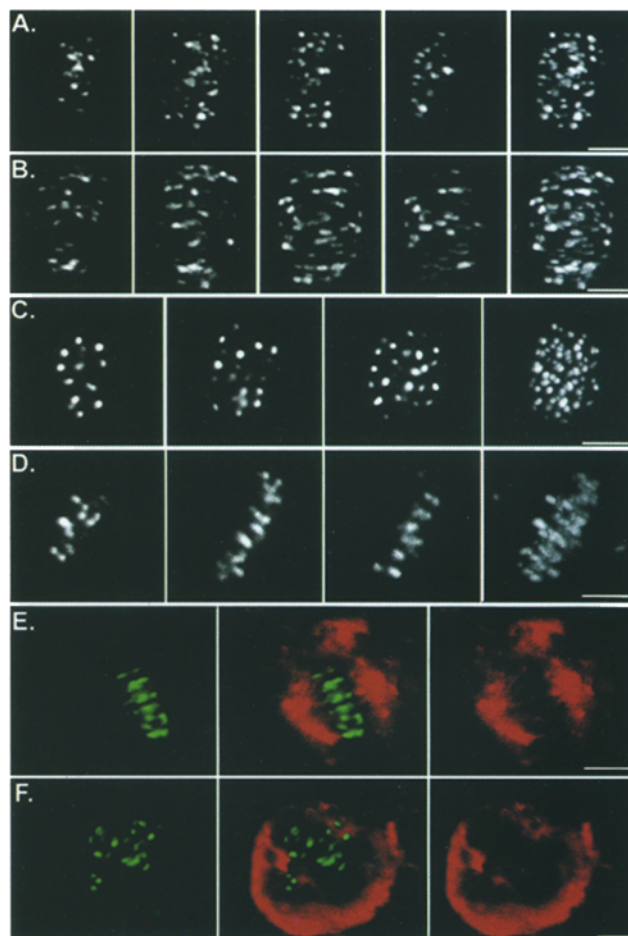


Figure 5. Mitotic  $\alpha$ -satellite elongation requires microtubules. Serial section confocal microscopy was used to examine  $\alpha$ -satellite morphology in cells arrested in mitosis with vinblastine (A, C, and E–F) and untreated mitotic cells (B and D). (A) Vinblastine-arrested cell fixed with 4% formaldehyde. The rightmost panel shows a projection of the complete optical section series while the four panels at left show successive projections of  $\sim 2$ - $\mu\text{m}$  segments of the series. (B) Prometaphase cell fixed and displayed as in A. (C) Live vinblastine-arrested cell showing whole cell projection in rightmost panel and three representative sections in the left panels. (D) Live metaphase cell displayed as in C. (E and F) Tubulin immunofluorescence was performed in order to examine residual spindle microtubule structures in vinblastine-arrested cultures after transfection with pCENPB-GFP. GFP (green) and tubulin (red) were simultaneously visualized by confocal microscopy. Note residual spindle structure in a cell with elongated centromeres (E) and the lack of detectable filamentous tubulin in a cell with symmetric centromeres (F). Scale bars equal 5 microns.

ected with cationic lipids and then treated with vinblastine is less than ideal, cells with detectable spindle remnants exhibited elongated centromere morphology (Fig. 5 E). In contrast, cells with symmetric centromeres lacked detectable spindle microtubules, although the metaphase-like organization of chromosomes was evident by exclusion of background tubulin staining (Fig. 5 F). Taken together, these observations show that the elongated morphology of  $\alpha$ -satellite domains at metaphase is closely correlated with the presence of spindle microtubules and thus is related to microtubule function in the spindle rather than mitotic chromosome structure per se.

### Time Lapse Observations of Centromere Morphology in Live Mitotic Cells

Chromosomes that have achieved bipolar attachment to the spindle are under tension across their centromeres (Nicklas, 1988) and undergo nearly continuous motility in the form of poleward-antipoleward oscillations around the metaphase plate (Skibbens et al., 1993). This motility was readily observed in cells transformed with CENPB-GFP using time lapse confocal microscopy (Fig. 6). During these oscillatory motions well resolved centromeres were occasionally observed undergoing apparent elastic distortion as the two sister satellite domains transiently separated from each other, in the direction of the spindle axis (arrows, Fig. 6 A). For quantitative analysis of these apparent elastic episodes, we measured the center-to-center distance between the paired fluorescent foci of two centromeres in this cell, plotted as a function of time in Fig. 6 B. The center-to-center distance, which measures the distance across the interior compartment of the centromere, increased from 0.6  $\mu\text{m}$  to 1  $\mu\text{m}$  in one case and from 0.75  $\mu\text{m}$  to 1.05  $\mu\text{m}$  in the other, a distortion of 0.3–0.4  $\mu\text{m}$ . These data show that the interior of the centromere, the central pairing domain and its surrounding heterochromatin, is a compliant element that reversibly expands along the direc-

tion of the spindle axis during metaphase chromosome oscillations.

### Tracking Centromere Motility in Mitosis and Interphase

During anaphase, the motility of centromeres can be tracked with CENPB-GFP for high resolution analysis of chromosome segregation (Fig. 7). We have successfully tracked up to 12 centromeres in a single plane through anaphase, allowing determination of both mean rates of poleward migration as well as observation of individual centromere behaviors. Centromeres in anaphase HeLa cells occasionally reverse their poleward migration and migrate toward the spindle equator for periods of 30–60 s (Fig. 7 A), as described for newt lung cells (Skibbens et al., 1993). During the recovery phase of these excursions, which we have observed in four anaphase HeLa cells, centromeres migrate at a rate that is 2–3-fold faster than the average rate of anaphase chromosome movement until they rejoin the moving chromosomal plate and resume a normal rate of migration (Fig. 7 B). This suggests that the anaphase governor, postulated to account for the slow rate of anaphase chromosome motility (Nicklas, 1983; for review see Inoue and Salmon, 1995), does not operate uniformly throughout the spindle but appears to be associated with chromosomes.

During telophase, the interphase nucleus is reformed by reassembly of the nuclear envelope and decondensation of the chromosomes. Time lapse series were collected beginning in late anaphase for periods up to 2 h, to visualize centromere behavior during telophase and early G1 (Fig. 8). Expansion of the tightly packed polar band of centromeres began almost immediately following cytokinesis and continued for up to 1 1/2 h. During this time the centromeres expanded radially, away from the center of the band in what appears as a nearly isometric expansion. Centromeres themselves did not decondense to a significant extent, consistent with their constitutive heterochro-

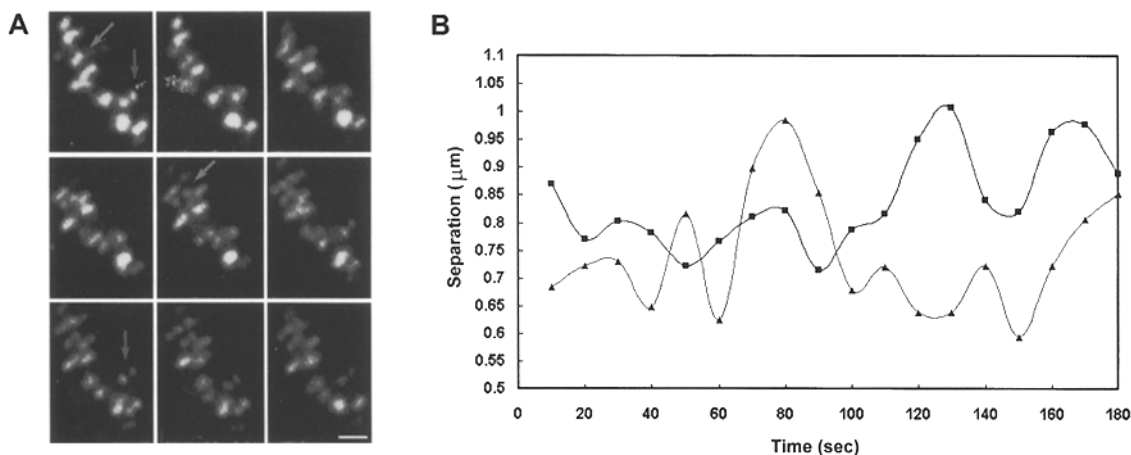


**Figure 6.** Apparent elastic behavior of  $\alpha$ -satellite domains in vivo. HeLa cells transfected with pCENPB-GFP were maintained in a perfusion chamber at 37°C for time lapse observation by confocal microscopy. Images were collected from a single plane at a rate of six frames per minute. (A) Images of a cell in metaphase are shown at 20-s intervals. Two centromeres that undergo apparent elastic distortions during metaphase oscillations are highlighted by arrows. Thick arrows are used at the start of the sequence (upper right) and at the time of maximal centromere extension. (B) The center-to-center distances between the paired sister  $\alpha$ -satellite domains of the two centromeres indicated in A are plotted as a function of time. Bar, (A) 2  $\mu\text{m}$ .

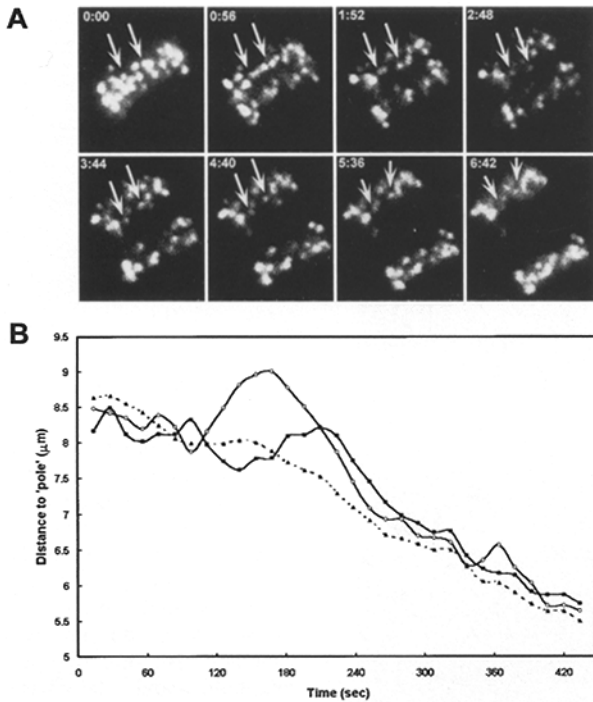


**Figure 7.** Anaphase governor activity does not operate uniformly throughout the spindle. Single plane confocal time lapse images were collected as in Fig. 6 at 12-s intervals for a cell executing anaphase. (A) Individual centromeres (arrows) were occasionally seen to reverse their poleward motion and migrate toward the spindle midzone for 40–60 s. (B) The distances between centromeres and fixed points approximating the spindle poles were determined and are plotted as a function of time. Dashed line, average distance for 12 centromeres; solid lines, centromere-to-pole distance for two oscillating centromeres shown in A. Centromeres in the recovery phase of anaphase oscillations moved faster than those closer to the pole.

matic nature. We did not observe any relative movement of centromeres in directions contrary to the overall expansion, although they showed more small scale (1–2  $\mu\text{m}$  radius) brownian-like motion than observed in mature nuclei. These data show that the position of each centromere within the early G1 nucleus is determined primarily by its position within the polar band, presumably dictated by patterns of decondensation of the chromosome arms.

Centromere dynamics during interphase have been inferred on the basis of changes in their patterns of distribution within the nucleus, detected by immunocytochemistry and in situ hybridization (e.g., Manuelidis, 1984, 1985; Ferguson and Ward, 1992; Janevski et al., 1995). Motile behavior of discrete genomic loci, however, has not been observed directly in living cells. During interphase we have observed fields of cells for up to 2 h at sampling rates of 1 frame per minute. The majority of centromeres observed in interphase nuclei remained at rest in fixed relative positions within the nucleus even as the nuclei moved as a result of cell locomotion. Essentially no brownian movement of centromeres was observed, although larger cytoplasmic or extracellular particles showed significant brownian motion, indicating that interphase chromatin acts as a relatively rigid matrix. Occasionally, however, we observed

motility of one or a few centromeres within an interphase nucleus (Fig. 9). These movements were very slow, on the order of 7–10  $\mu\text{m}$  per hour, and appeared to be specific motility of certain centromeres, since nearby centromeres remained motionless during the observation period. Thus, movement of centromeres within the nucleus after telophase occurs relatively infrequently but does occur in an apparently selective fashion.

## Discussion

In vivo labeling of centromere DNA sequences using a fluorescent CENP-B derivative provides a novel approach for investigation of chromosome dynamics at all stages of the cell cycle. The target site for CENP-B binding is a 17-bp sequence found within the 170-bp  $\alpha$ -satellite monomer that comprises the basic repeat unit for the large tandem arrays of alphoid DNA present in human centromeres (Masumoto et al., 1989). While the abundance of CENP-B box sequences in human DNA has not been directly measured,  $\sim 10\%$  of sequenced  $\alpha$ -satellite monomers in GenBank possess a CENP-B box, which would correspond to  $\sim 3,000$  sites per chromosome, on average. Estimates of CENP-B abundance in HeLa cells range from  $\sim 300$ – $600$  copies per chromosome (Earnshaw, W.C., personal communication and Sullivan, K.F., unpublished observations). From these estimates, it would appear that  $\alpha$ -satellite loci are not saturated by endogenous CENP-B. In immunofluorescence experiments, CENPB-GFP transfected cells often appeared brighter than surrounding cells using a human anti-centromere serum that recognizes the CENP-B DNA-binding domain, indicating that HeLa centromeres do in fact have a capacity to incorporate additional CENP-B. We estimate that the signals we observe correspond to 300–3,000 GFP molecules per centromere, on average.

Elongation of centromeres at metaphase is observed using both intrinsic staining with CENPB-GFP as well as immunofluorescence with mACA-1. However, in contrast to mACA-1 staining, which readily resolves the paired spots of sister centromeres at metaphase, CENPB-GFP fluorescence often appears continuous across the centromere. We believe this is due to increased sensitivity of detection of  $\alpha$ -satellite DNA with CENPB-GFP, due in part to overexpression and increased occupancy of the available CENP-B box sequences. Our results with CENPB-GFP are consistent with those of Cooke and Earnshaw (1990) who reported that CENP-B is localized broadly throughout the heterochromatic domain of the centromere, based on immunoelectron microscopy. On many human chromosomes, contiguous blocks of  $\alpha$ -satellite DNA comprise most, if not all, of the cytogenetically defined centromere (Tyler-Smith and Brown, 1987; Tyler-Smith and Willard, 1993), although these arrays can be punctuated by non- $\alpha$ -satellite sequences on some chromosomes (Wevrick et al., 1992). Two distinct  $\alpha$ -satellite arrays are found on both chromosomes 7 (Wevrick et al., 1992; Haaf and Ward, 1994) and 21 (Ikeno et al., 1994), and in both cases the primary constriction is comprised of a CENP-B box rich  $\alpha$ -satellite subfamily. Taken together, these observations are consistent with the idea that the primary constriction is comprised of  $\alpha$ -satellite DNA with a high density of CENP-B-binding sites which we can label to high occu-

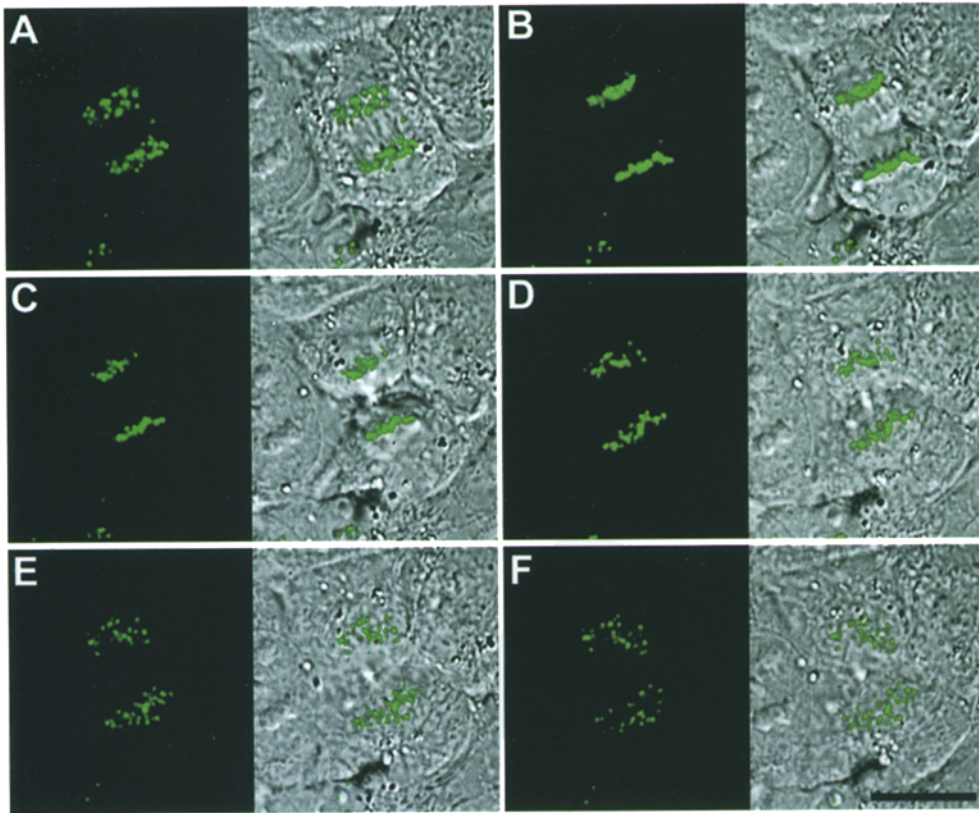


**Figure 8.** Centromere dispersal at telophase appears as a nearly isometric expansion. A time lapse sequence was collected from a U2OS (human osteosarcoma) cell transfected with CENPB-GFP, beginning in late anaphase. Successive images are shown at 5-min intervals spanning 30 min of late anaphase and telophase. CENPB-GFP fluorescence is shown at left with a reflectance mode image on the right in each panel. Bar, 10  $\mu\text{m}$ .

pancy, resulting in the continuous fluorescent signals typically seen at GFP-labeled HeLa centromeres.

Evidence that kinetochores are able to stretch during mitosis comes from early light and electron microscopy of mitotic cells as well as more recent video DIC techniques (Roos, 1973; Tippit et al., 1980; Rieder and Borisy, 1981; Skibbens et al., 1993). During prometaphase in mammalian cells, kinetochores bound to microtubule fibers can often be seen stretched toward a pole, attached by a thin strand drawn out from the chromosome. This is dramatically observed in diatoms, where sister kinetochores stretch to opposite poles by metaphase (Tippit et al., 1980), but kinetochores appear more relaxed by metaphase in animal cells (Roos, 1973; McIntosh et al., 1975; Rieder and Borisy, 1981). Indeed, many electron microscopic images give the impression that the central region of the chromosome is resistant to deformation (e.g., Figs. 3 and 7 of Roos, 1973). The elongation of  $\alpha$ -satellite domains appears to differ from this kinetochore stretching, as it involves the central domain of the centromere and does not become maximal until metaphase. Nevertheless, the microtubule dependence of this process suggests that it is driven by spindle forces and reports on the tension, or net force, exerted across the centromere.

If  $\alpha$ -satellite comprises the DNA of the primary constriction, then what is the space between separated CENP-B foci? One possibility is that sequences flanking the  $\alpha$ -satellite domains could be folded to form the interior part of the centromere, similar to the model for interaction of flanking elements of the *S. pombe* centromere with the central core sequences (Marschall and Clarke, 1995). This seems unlikely since loci flanking CENP-B rich  $\alpha$ -satellite domains appear peripheral to the primary constriction by

in situ hybridization (Ikeno et al., 1994; Haaf and Ward, 1994). Available data, however, do not formally rule out the possibility that  $\alpha$ -satellite could contain other sequence classes interspersed within the arrays, as observed in *Drosophila* centromere associated satellite arrays (Le et al., 1995). The space could represent a transient separation of the chromatids at the primary constriction. Experimental integration of  $\alpha$ -satellite DNA arrays into nonhuman chromosomes produces aberrant chromatid cohesion in anaphase, suggesting a role for  $\alpha$ -satellite in maintaining the connection across the centromere (Haaf et al., 1992; Larin et al., 1994). Occasionally, however, the chromatin of the inner centromere region of metaphase chromosomes does appear to be extended and less dense than the surrounding chromatin (Roos, 1973; McIntosh et al., 1975; Skibbens et al., 1993). A third alternative is that the space represents a nonchromatin component that links the two chromatids. While it is clear that chromatid cohesion at the centromere is ultimately protein dependent (Holloway et al., 1993; Stratmann and Lehner, 1996), there is no evidence for a large nonchromatin component of the central pairing domain of the centromere. Rather, in examples of extended metaphase centromeres, the material linking the two chromatids appears identical to the surrounding chromatin fibers. We favor the hypotheses that either CENP-B is excluded from this region through assembly of other centromere proteins or that the chromatin fibers between sister chromatids becomes drawn to a point where CENP-B falls below detectable levels. In either case, the separation of CENP-B foci reveals an elastic element at the center of the centromere that is almost certainly comprised of some form of  $\alpha$ -satellite chromatin.

The late timing and interior location of the central do-

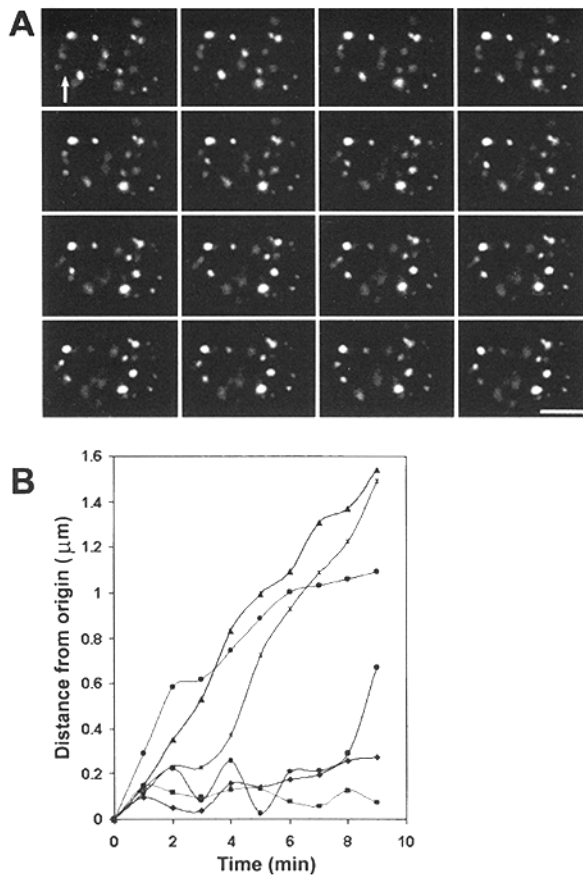


**Figure 9.** Localized motility of  $\alpha$ -satellite domains in interphase nuclei. A single plane confocal time lapse series was collected as in Fig. 6 at 30-s intervals for a field of interphase cells. Significant centromere motility was observed in one of five cells observed over a 1-h period. (A) Successive images, progressing from top left to bottom right, from a cell exhibiting interphase centromere motility, with an arrow indicating the region of interest. (B) Interphase centromere movement is plotted as the distance from the starting position for a group of six centromeres from the region indicated in panel A. Three centromeres exhibit motility while three centromeres in the same vicinity of the nucleus remain relatively stationary throughout the interval shown.

main elasticity we observe indicates that it is, at least partially, distinct from the poleward stretching of chromatin subjacent to the kinetochore that occurs during prometaphase. This could be due to different elastic properties of the two chromatin compartments or to some viscoelastic property of the  $\alpha$ -satellite chromatin. In this respect it is important to note that tension appears to regulate different kinds of activities during mitosis. The anaphase checkpoint detects a low frequency event, bipolar chromosome attachment, that occurs only once for each chromosome in mitosis (Nicklas and Ward, 1994) and acts globally throughout the cell. Conversely, the rapid reversals of kinetochore motility exhibited by oscillating chromosomes occur at high frequency throughout mitosis and act locally on individual kinetochores (Skibbens et al., 1993, 1995). The presence of multiple elastic components within the centromere could be a way for the spindle to isolate different mechanical signaling mechanisms of the

chromosomes, or buffer the communication between sister kinetochores.

Despite the normal correlation between  $\alpha$ -satellite DNA and the functional centromere,  $\alpha$ -satellites are highly polymorphic (Wevrick and Willard, 1989; Tyler-Smith et al., 1993) and instances of centromeres that possess no detectable  $\alpha$ -satellite DNA have been reported (Voullaire et al., 1993; Blennow et al., 1994). Chromosomes without detectable levels of  $\alpha$ -satellite DNA sometimes segregate normally (Voullaire et al., 1993) but sometimes do not (Blennow et al., 1994). How is this consistent with any definite role for  $\alpha$ -satellite DNA? In centromeres devoid of  $\alpha$ -satellite DNA or CENP-B, other conserved centromere proteins may be present at the functional centromere, including CENP-A (Voullaire et al., 1993) and CENP-C (Earnshaw et al., 1989), perhaps in association with a normally inactive latent centromere locus. Dissection of a *Drosophila* centromere resulted in construction of acentric chromosome derivatives that, although lacking the essential central core sequences, retained some segregation capability (Murphy and Karpen, 1995). In *S. pombe*, an epigenetic feature of centromere function has been identified that is correlated with the unique chromatin structure of the central core of the centromere (Steiner and Clarke, 1994). In these experiments, cells could spontaneously activate defective centromeres in the absence of any change at the level of DNA sequence. These results suggest that some important functions of the centromere are dependent on the unique features of centromeric chromatin and perhaps partially independent of the underlying DNA sequences.

The positions of centromeres in interphase reflect the underlying distribution of chromosomes within the nucleus. Previous experiments indicate that chromosomes occupy essentially random positions in the nuclei of cultured mammalian cells (Lichter et al., 1988), consistent with a largely stochastic mechanism for reassembling the interphase nucleus after mitosis. We observe a rapid dispersal of centromeres during telophase and early G<sub>1</sub>, which appears as a nearly isometric expansion driven, presumably, by chromosome decondensation. The resulting position of a particular centromere within the nucleus depends on its precise position at the end of anaphase and on patterns of chromosome decondensation (Hiraoka et al., 1989). Nevertheless, centromere distribution in interphase may be correlated with functional states of the cell (Pluta et al., 1995) and the notion that chromosomes adopt functionally important spatial arrangements within the nucleus has been a significant focus of modern cytogenetics (e.g., Haaf and Schmid, 1991; Cremer et al., 1993). Centromere distribution changes as a function of differentiation, the cell cycle and in response to transcriptional signals (Manuelidis, 1984; Bartholdi, 1991; Ferguson and Ward, 1992; Funabiki et al., 1993; Janevski et al., 1995), suggesting that mechanisms operating during interphase can move chromosomes or chromosome domains. Detection of a cell cycle-dependent association of human chromosome 15 homologues occurring in late S-phase demonstrates that these mechanisms can act at the level of specific chromosomes (Lalande and LaSalle, 1996). The slow movements of centromeres that we have observed in interphase could be a reflection of chromosomal transport mechanisms that

mediate the dynamic functional arrangement of chromosomes within the nucleus.

Although the mechanisms that mediate chromosome motility in interphase are not known, it has become clear that nuclei contain numerous mechanochemical activities, not least of which are the polymerases that transcribe and replicate DNA (Yin et al., 1995). A new family of putative ATPases, the SMC proteins, function in diverse nuclear events including dosage compensation, chromosome condensation, and centromere function (Strunnikov et al., 1993; Hirano and Mitchison, 1994; Hirano et al., 1995). It has been suggested that these proteins comprise a class of chromosomal motors that serve the mechanical requirements of the nucleus. It is not clear whether the motility of interphase centromeres we have observed arises from directed motility processes or indirectly through changes in chromosome structure or activity. However, the ability to observe specific DNA sequence domains in living nuclei provides a powerful assay tool that should prove useful for dissecting the molecular mechanisms underlying the dynamic spatial organization of the genome.

We thank J. Harper, R. Heim, and R. Tsien for providing GFP plasmids, L. Gerace and C. Fritze for lamin-A antiserum. We are also grateful to B.M. Schwartz and M. Pique for help with animation of timelapse data.

This work was supported in part by a grant from the National Institutes of Health to K.F. Sullivan, and by a grant from the Markey Charitable Trust to the Department of Cell Biology.

Received for publication 11 June 1996 and in revised form 12 August 1996.

## References

- Ault, J.G., and R.B. Nicklas. 1989. Tension, microtubule rearrangements, and the proper distribution of chromosomes in mitosis. *Chromosoma*. 98:33-39.
- Bartholdi, M.F. 1991. Nuclear distribution of centromeres during the cell cycle of human diploid fibroblasts. *J. Cell Sci.* 99:255-263.
- Blennow, E., H. Telenius, D. de Vos, C. Larsson, P. Henriksson, O. Johansson, N.P. Carter, and M. Nordenskjöld. 1994. Tetrasomy 15q: two marker chromosomes with no detectable  $\alpha$ -satellite DNA. *Am. J. Hum. Gen.* 54:877-883.
- Bloom, K.S., E. Amaya, J. Carbon, L. Clarke, A. Hill, and E. Yeh. 1984. Chromatin conformation of yeast centromeres. *J. Cell Biol.* 99:1559-1568.
- Brenner, S., D. Pepper, M.W. Berns, E. Tan, and B.R. Brinkley. 1981. Kinetochores structure, duplication, and distribution in mammalian cells: analysis by human autoantibodies from scleroderma patients. *J. Cell Biol.* 91:95-102.
- Chalfie, M., Y. Tu, G. Euskirchen, W.W. Ward, and D.C. Prasher. 1994. Green fluorescent protein as a marker for gene expression. *Science (Wash. DC)*. 263:802-805.
- Clarke, L., and J. Carbon. 1980. Isolation of a yeast centromere and construction of functional small circular chromosomes. *Nature (Lond.)*. 287:504-509.
- Compton, D.A., T.J. Yen, and D.W. Cleveland. 1991. Identification of novel centromere/kinetochore-associated proteins using monoclonal antibodies generated against human mitotic chromosome scaffolds. *J. Cell Biol.* 112:1083-1097.
- Cooke, C.A., R.L. Bernat, and W.C. Earnshaw. 1990. CENP-B: a major human centromere protein located beneath the kinetochore. *J. Cell Biol.* 110:1475-1488.
- Cremer, T., A. Kurz, R. Zirbel, S. Dietzel, B. Rinke, E. Schrock, M.R. Speicher, U. Mathieu, A. Jauch, P. Emmerich et al. 1993. Role of chromosome territories in the functional compartmentalization of the cell nucleus. *Cold Spring Harb. Symp. Quant. Biol.* 58:777-792.
- Cyert, M.S., T. Scherson, and M.W. Kirschner. 1988. Monoclonal antibodies specific for thiophosphorylated proteins recognize *Xenopus* MPF. *Dev. Biol.* 129:209-216.
- Earnshaw, W.C., and J.B. Rattner. 1989. A map of the centromere (primary constriction) in vertebrate chromosomes at metaphase. *Prog. Clin. & Biol. Res.* 318:33-42.
- Earnshaw, W.C., K.F. Sullivan, P.S. Machlin, C.A. Cooke, D.A. Kaiser, T.D. Pollard, N.F. Rothfield, and D.W. Cleveland. 1987. Molecular cloning of cDNA for CENP-B, the major human centromere autoantigen. *J. Cell Biol.* 104:817-829.
- Earnshaw, W.C., H. Ratrie, and G. Stetten. 1989. Visualization of centromere proteins CENP-B and CENP-C on a stable dicentric chromosome in cytological spreads. *Chromosoma*. 98:1-12.
- Ferguson, M., and D.C. Ward. 1992. Cell cycle dependent chromosomal movement in pre-mitotic human T-lymphocyte nuclei. *Chromosoma*. 101:557-565.
- Funabiki, H., I. Hagan, S. Uzawa, and M. Yanagida. 1993. Cell cycle-dependent specific positioning and clustering of centromeres and telomeres in fission yeast. *J. Cell Biol.* 121:961-976.
- Gimenez-Abian, J.F., D.J. Clarke, A.M. Mullinger, C.S. Downes, and R.T. Johnson. 1995. A postprophase topoisomerase II-dependent chromatid core separation step in the formation of metaphase chromosomes. *J. Cell Biol.* 131:7-17.
- Gorbsky, G.J., and W.A. Ricketts. 1993. Differential expression of a phosphoepitope at the kinetochores of moving chromosomes. *J. Cell Biol.* 122:1311-1321.
- Haaf, T., and M. Schmid. 1991. Chromosome topology in mammalian interphase nuclei. *Exp. Cell Res.* 192:325-332.
- Haaf, T., and D.C. Ward. 1994. Structural analysis of  $\alpha$ -satellite DNA and centromere proteins using extended chromatin and chromosomes. *Hum. Mol. Genet.* 3:697-709.
- Haaf, T., P.E. Warburton, and H.F. Willard. 1992. Integration of human  $\alpha$ -satellite DNA into simian chromosomes: centromere protein binding and disruption of normal chromosome segregation. *Cell*. 70:681-696.
- Hirano, T., and T.J. Mitchison. 1994. A heterodimeric coiled-coil protein required for mitotic chromosome condensation in vitro. *Cell*. 79:449-458.
- Hirano, T., T.J. Mitchison, and J.R. Swedlow. 1995. The SMC family: from chromosome condensation to dosage compensation. *Curr. Opin. Cell Biol.* 7:329-336.
- Hiraoka, Y., J.S. Minden, J.R. Swedlow, J.W. Sedat, and D.A. Agard. 1989. Focal points for chromosome condensation and decondensation revealed by three-dimensional in vivo time-lapse microscopy. *Nature (Lond.)*. 342:293-296.
- Hiraoka, Y., J.W. Sedat, and D.A. Agard. 1990. Determination of three-dimensional imaging properties of a light microscope system. Partial confocal behavior in epifluorescence microscopy. *Biophys. J.* 57:325-333.
- Holloway, S.L., M. Glotzer, R.W. King, and A.W. Murray. 1993. Anaphase is initiated by proteolysis rather than by the inactivation of maturation-promoting factor. *Cell*. 73:1393-1402.
- Hyman, A.A., and T.J. Mitchison. 1990. Modulation of microtubule stability by kinetochores in vitro. *J. Cell Biol.* 110:1607-1616.
- Hyman, A.A., and T.J. Mitchison. 1991. Two different microtubule-based motor activities with opposite polarities in kinetochores. *Nature (Lond.)*. 351:206-211.
- Ikeno, M., H. Masumoto, and T. Okazaki. 1994. Distribution of CENP-B boxes reflected in CREST centromere antigenic sites on long-range  $\alpha$ -satellite DNA arrays of human chromosome 21. *Hum. Mol. Genet.* 3:1245-1257.
- Inoue, S., and E.D. Salmon. 1995. Force generation by microtubule assembly/disassembly in mitosis and related movements. *Mol. Biol. Cell*. 6:1619-1640.
- Janevski, J., P.C. Park, and U. De Boni. 1995. Organization of centromeric domains in hepatocyte nuclei: rearrangement associated with de novo activation of the vitellogenin gene family in *Xenopus laevis*. *Exp. Cell Res.* 217:227-239.
- Jordan, M.A., D. Thrower, and L. Wilson. 1992. Effects of vinblastine, podophyllotoxin and nocodazole on mitotic spindles. Implications for the role of microtubule dynamics in mitosis. *J. Cell Sci.* 102:401-416.
- Lalonde, M., and J.M. LaSalle. 1996. Homologous association of oppositely imprinted chromosomal domains. *Science (Wash. DC)*. 272:725-728.
- Larin, Z., M.D. Fricker, and C. Tyler-Smith. 1994. De novo formation of several features of a centromere following introduction of a Y alphoid YAC into mammalian cells. *Hum. Mol. Gen.* 3:689-695.
- Le, M.H., D. Duricka, and G.H. Karpen. 1995. Islands of complex DNA are widespread in *Drosophila* centric heterochromatin. *Genetics*. 141:283-303.
- Lichter, P., T. Cremer, J. Borden, L. Manuelidis, and D.C. Ward. 1988. Delineation of individual human chromosomes in metaphase and interphase cells by in situ suppression hybridization using recombinant DNA libraries. *Hum. Genet.* 80:224-234.
- Li, X., and R.B. Nicklas. 1995. Mitotic forces control a cell-cycle checkpoint. *Nature (Lond.)*. 373:630-632.
- Liao, H., R.J. Winkfein, G. Mack, J.B. Rattner, and T.J. Yen. 1995. CENP-F is a protein of the nuclear matrix that assembles onto kinetochores at late G2 and is rapidly degraded after mitosis. *J. Cell Biol.* 130:507-518.
- Lombillo, V.A., R.J. Stewart, and J.R. McIntosh. 1995. Minus-end-directed motion of kinesin-coated microspheres driven by microtubule depolymerization. *Nature (Lond.)*. 373:161-164.
- Manuelidis, L. 1984. Different central nervous system cell types display distinct and nonrandom arrangements of satellite DNA sequences. *Proc. Natl. Acad. Sci. USA*. 81:3123-3127.
- Manuelidis, L. 1985. Indications of centromere movement during interphase and differentiation. *Ann. NY. Acad. Sci.* 450:205-221.
- Marschall, L.G., and L. Clarke. 1995. A novel *cis*-acting centromeric DNA element affects *S. pombe* centromeric chromatin structure at a distance. *J. Cell Biol.* 128:445-454.
- Masumoto, H., H. Masukata, Y. Muro, N. Nozaki, and T. Okazaki. 1989. A human centromere antigen (CENP-B) interacts with a short specific sequence in alphoid DNA, a human centromeric satellite. *J. Cell Biol.* 109:1963-1973.
- McIntosh, J.R. 1991. Structural and mechanical control of mitotic progression. *Cold Spring Harbor Symp. Quant. Biol.* 56:613-619.
- McIntosh, J.R., Z.W. Cande, and J.A. Snyder. 1975. Structure and physiology of the mammalian mitotic spindle. In *Molecules and Cell Movement*. S. Inoué and R.E. Stephens, editors. Raven Press, New York. pp. 31-76.

- Mitchison, T.J., and M.W. Kirschner. 1985. Properties of the kinetochore in vitro. II. Microtubule capture and ATP-dependent translocation. *J. Cell Biol.* 101:766-777.
- Murphy, T.D., and G.H. Karpen. 1995. Localization of centromere function in a *Drosophila* minichromosome. *Cell.* 82:599-609.
- Nicklas, R.B. 1983. Measurements of the force produced by the mitotic spindle in anaphase. *J. Cell Biol.* 97:542-548.
- Nicklas, R.B. 1988. The forces that move chromosomes in mitosis. *Annu. Rev. Biophys. Biophys. Chem.* 17:431-449.
- Nicklas, R.B., and S.C. Ward. 1994. Elements of error correction in mitosis: microtubule capture, release, and tension. *J. Cell Biol.* 126:1241-1253.
- Nicklas, R.B., S.C. Ward, and G.J. Gorbsky. 1995. Kinetochore chemistry is sensitive to tension and may link mitotic forces to a cell cycle checkpoint. *J. Cell Biol.* 130:929-939.
- Pluta, A.F., N. Saitoh, I. Goldberg, and W.C. Earnshaw. 1992. Identification of a subdomain of CENP-B that is necessary and sufficient for localization to the human centromere. *J. Cell Biol.* 116:1081-1093.
- Pluta, A.F., A.M. Mackay, A.M. Ainsztein, I.G. Goldberg, and W.C. Earnshaw. 1995. The centromere: hub of chromosomal activities. *Science (Wash. DC)*. 270:1591-1594.
- Polizzi, C., and L. Clarke. 1991. The chromatin structure of centromeres from fission yeast: differentiation of the central core that correlates with function. *J. Cell Biol.* 112:191-201.
- Prasher, D.C., V.K. Eckenrode, W.W. Ward, F.G. Prendergast, and M.J. Cormier. 1992. Primary structure of the *Aequorea victoria* green-fluorescent protein. *Gene (Amst.)*. 111:229-233.
- Rieder, C.L., and G.G. Borisy. 1981. The attachment of kinetochores to the pro-metaphase spindle in PtK1 cells. Recovery from low temperature treatment. *Chromosoma*. 82:693-716.
- Rieder, C.L., A. Schultz, R. Cole, and G. Sluder. 1994. Anaphase onset in vertebrate somatic cells is controlled by a checkpoint that monitors sister kinetochore attachment to the spindle. *J. Cell Biol.* 127:1301-1310.
- Rieder, C.L., R.W. Cole, A. Khodjakov, and G. Sluder. 1995. The checkpoint delaying anaphase in response to chromosome monoorientation is mediated by an inhibitory signal produced by unattached kinetochores. *J. Cell Biol.* 130:941-948.
- Roos, U.P. 1973. Light and electron microscopy of rat kangaroo cells in mitosis. II. Kinetochore structure and function. *Chromosoma*. 41:195-220.
- Skibbens, R.V., V.P. Skeen, and E.D. Salmon. 1993. Directional instability of kinetochore motility during chromosome congression and segregation in mitotic newt lung cells: a push-pull mechanism. *J. Cell Biol.* 122:859-875.
- Skibbens, R., C.L. Rieder, and E.D. Salmon. 1995. Kinetochore motility after severing between sister chromosomes using laser microsurgery: evidence that kinetochore directional instability and position is regulated by tension. *J. Cell Sci.* 108:2537-2548.
- Steiner, N.C., and L. Clarke. 1994. A novel epigenetic effect can alter centromere function in fission yeast. *Cell*. 79:865-874.
- Stratmann, R., and C.F. Lehner. 1996. Separation of sister chromatids in mitosis requires the *Drosophila* pimpls product, a protein degraded after the metaphase/anaphase transition. *Cell*. 84:25-35.
- Strunnikov, A.V., V.L. Larionov, and D. Koshland. 1993. SMC1: an essential yeast gene encoding a putative head-rod-tail protein is required for nuclear division and defines a new ubiquitous protein family. *J. Cell Biol.* 123:1635-1648.
- Sullivan, K.F., and C.A. Glass. 1991. CENP-B is a highly conserved mammalian centromere protein with homology to the helix-loop-helix family of proteins. *Chromosoma*. 100:360-370.
- Sullivan, K.F., M. Hechenberger, and K. Masri. 1994. Human CENP-A contains a histone H3 related histone fold domain that is required for targeting to the centromere. *J. Cell Biol.* 127:581-592.
- Tippit, D.H., J.D. Pickett-Heaps, and R. Leslie. 1980. Cell division in two large pennate diatoms *Hantzschia* and *Nitzschia* III. A new proposal for kinetochore function during prometaphase. *J. Cell Biol.* 86:402-416.
- Tyler-Smith, C., and W.R. Brown. 1987. Structure of the major block of alphoid satellite DNA on the human Y chromosome. *J. Mol. Biol.* 195:457-470.
- Tyler-Smith, C., and H.F. Willard. 1993. Mammalian chromosome structure. *Curr. Opin. Genet. Dev.* 3:390-397.
- Tyler-Smith, C., R.J. Oakey, Z. Larin, R.B. Fisher, M. Crocker, N.A. Affara, M.A. Ferguson-Smith, M. Muenke, O. Zuffardi, and M.A. Jobling. 1993. Localization of DNA sequences required for human centromere function through an analysis of rearranged Y chromosomes. *Nature Genet.* 5:368-375.
- Voullaire, L.E., H.R. Slater, V. Petrovic, and K.H. Choo. 1993. A functional marker centromere with no detectable  $\alpha$ -satellite, satellite III, or CENP-B protein: activation of a latent centromere? *Am. J. Hum. Gen.* 52:1153-1163.
- Wendell, K.L., L. Wilson, and M.A. Jordan. 1993. Mitotic block in HeLa cells by vinblastine: ultrastructural changes in kinetochore-microtubule attachment and in centrosomes. *J. Cell Sci.* 104:261-274.
- Wevrick, R., and H.F. Willard. 1989. Long-range organization of tandem arrays of  $\alpha$ -satellite DNA at the centromeres of human chromosomes: high-frequency array-length polymorphism and meiotic stability. *Proc. Natl. Acad. Sci. USA*. 86:9394-9398.
- Wevrick, R., V.P. Willard, and H.F. Willard. 1992. Structure of DNA near long tandem arrays of  $\alpha$ -satellite DNA at the centromere of human chromosome 7. *Genomics*. 14:912-923.
- Willard, H.F. 1991. Evolution of  $\alpha$ -satellite. *Curr. Opin. Genet. Dev.* 1:509-514.
- Yen, T.J., G. Li, B.T. Schaar, I. Szilak, and D.W. Cleveland. 1992. CENP-E is a putative kinetochore motor that accumulates just before mitosis. *Nature (Lond.)*. 359:536-539.
- Yin, H., M.D. Wang, K. Svoboda, R. Landick, S.M. Block, and J. Gelles. 1995. Transcription against an applied force. *Science (Wash. DC)*. 270:1653-1657.
- Yoda, K., K. Kitagawa, H. Masumoto, Y. Muro, and T. Okazaki. 1992. A human centromere protein, CENP-B, has a DNA binding domain containing four potential  $\alpha$ -helices at the NH<sub>2</sub> terminus, which is separable from dimerizing activity. *J. Cell Biol.* 119:1413-1427.